Design and validation of an actuation mechanism designed for controlled DRS probe insertion for bone sensing in vertebra pedicle

B. Cleijpool (4581369), T.K. Scheepstra (4593162),
A.W. Schurink (4631242), P.I. van der Stigchel (4588010),
J.G. Verkerk (4562747)

***Abstract*— Currently, an estimated 20% of pedicle screws placed during spinal fusion surgery are still being misplaced. Diffuse reflection spectroscopy (DRS) is a promising new technique used for measuring bone types and can potentially improve the success rate of screw placement. The goal of our project is to design, build and test an actuating system that can validate a DRS probe through controlled insertion into a pedicle of a vertebra. This insertion will be performed on a fixed isolated segment of spinal vertebrae. Controlled actuation is interpreted as a maximum step size of 1 mm, which is determined by the minimum thickness of cortical bone (0.5 mm) and the probe detection depth (0.5 mm). The probe has been implemented in a screwing mechanism that can be actuated by a stepper motor and a pneumatic cylinder. Actuation depth is measured with a laser sensor and the vertebrae are adaptably fixated using scharp pins and can adjustably positioned with a ball-joint clamp. Testing showed that an actuating step of 1 mm can be achieved at error margins of at least $+0\%$ and -3%, smaller actuating can also be used, consequently with higher error margins. Measurements of combined system deflection and backlash show that the probe will not break out of the pedicle during insertion. Readouts of DRS measurement show similar results during actuation compared to static reference measurements and the endured axial load by the probe and screw is an estimated 170 N.**

INTRODUCTION

Application of spinal fusion surgery has increased over the past decades. From 1998 up to 2008, the number of spinal fusion surgeries in the United States increased from 174,223 to 413,171 cases per year.[1] This increase can be accounted to the growing elderly population and the development of spinal fixation devices, however there are also cases in which younger patients need similar treatment. Spinal fusion surgery is applied when patients suffer diseases like scoliosis, arthrosis and other diseases or injuries that cause spinal instability.[2] The purpose of spinal fusion surgery is to merge multiple spinal vertebrae to regain spinal stability. By interconnecting the vertebrae with steel rods and screws, motion is terminated, causing the vertebrae to merge over time by growing bone tissue. The screws are usually placed through the pedicle of the vertebra, which contains a harder outer layer of cortical bone and a softer cancellous bone inside.

Insertion of the pedicle screws requires high accuracy and high precision. Due to the pedicle widcth of 4-16 mm [3] compared to the screw diameter of 4.5 to 7.0 mm [4], complications arise. If the screw is misplaced, the inner cortical wall might be breached, resulting in neurologic or vascular complications.[5] Several studies were conducted to identify the frequency of pedicle screw misplacement. Schulze et al.[6] found that experienced surgeons place 80 percent of the screws with less than 2 mm penetration of the pedicle wall, which is still acceptable. The other 20 percent was misplaced, penetrating the inner or outer cortical wall over 2 mm. Castro et al.[7] found that 29 percent of lumbar screw insertions penetrated the inner cortical wall of the pedicle and concluded that: *'Correct placement of transpedicular screws for spinal fusion seems to be more difficult than it looks.'*

Alternative to inserting the screw free-handedly[8], navigation methods are developed to aid the surgeon with precise insertion. Screw insertion with navigational techniques showed a higher accuracy rate compared to screw insertions with non-navigational techniques.[9][10] Two main navigational techniques are currently used; intraoperative fluoroscopy[11][12] and computer assisted surgery (CAS). Fluoroscopy uses X-ray images for navigation. Consequently, both the surgeon and the patient are exposed to radiation, which might lead to the growth of cancerous tumors.[13] CAS uses markers, sensors, and software to guide the surgeon, but research shows that only 11 percent of the surgeons uses CAS routinely, as application in their workflow has shown to be inconvenient.[14]

Another guidance system uses diffuse reflectance spectroscopy (DRS). DRS is a technique based on light interaction with material and can be used to measure bone type, the harder outer cortical bone or the softer cancellous inner bone. DRS can also measure bone type transition in real time and could therefore be used to alert the surgeon, if the screw approaches cortical bone with the spinal cord behind it. Implementation of DRS in spinal fusion surgery could result in a decrease of insertion time, radiation exposure, and revision surgery. Therefore, the system might be more applicable to the workflow of the surgeon.[15]

Based on this promising technique, TU Delft and Philips developed a DRS sensor; a long and tight shafted probe with an outer diameter of 2 mm and length of 179 mm, containing two fibers transporting the light. The DRS sensor can measure fat percentage in bone, which gives an indication for the type of bone and can even predict the distance to cortical bone.[15] The next step in the development of this

For questions or more information, please contact Akash Swamy: A.Swamy@tudelft.nl

technique will be to validate the DRS sensor (or probe) in an (automated) operational setup. An actuation mechanism is required to show that a controlled insertion of the DRS probe is possible, and to verify the results found by Swamy et al.[15]
Several (robotical) actuation mechanism already exist; Actuation systems that aid the surgeon with aiming or via a haptic interface[16][17][18], and actuation systems that are integrated with image navigation or computer assisted navigation like previously mentioned (CAS, fluoroscopy).[19][20][21] However, none of these actuation systems are applicable to the DRS sensor. Hence, this paper will cover the development of an actuation mechanism that focuses on the implementation of the DRS sensor. This ambition is translated into the next design goal: **Design and test an actuating mechanism that can drive the DRS probe into a vertebra pedicle.**
The paper will be guided by the following structure. Firstly, the system requirements will be explained in I. Secondly the design considerations will be elaborated in chapter II. Thirdly the requirement validation and result analysis are stated in chapter III and chapter IV respectively. Finally, study results will be discussed and concluded in chapters VI and VII. This design study has been conducted as part of the Bachelor End Project for Mechanical Engineering students at the TU Delft.

METHOD

I. REQUIREMENTS

Prior to designing the actuation system, a set of requirements was developed. These requirements can be sub divided into three groups: the actuation, fixation and the non functional requirements. These groups are presented next in order of significance.

A. Actuation

1) **2DOF (translate along one line and rotate around this axis) screwing/drilling mechanism to drive the DRS probe into bone tissue.** A screwing or drilling like mechanism is needed to achieve a highly controlled insertion into a vertebra, because of the heterogeneity within bone the insertion force is inconstant, so the probe cannot directly been inserted in a controlled fashion. .[22]
2) **The maximum step size of the actuating mechanism is 1.0 mm.** The maximum step size is determined by the thickness of the cortical bone in the vertebra and the properties of the DRS detection technique. The thickness of the cortical bone in the vertebra differs between persons and between locations within the vertebra. This thickness ranges from 0.5 mm to 3 mm. [23][24] Furthermore, the DRS probe has a detection depth of 0.5 mm from the tip. Therefore the maximum step size of 1 mm is required in order to prevent complete penetration of the cortical wall within one actuation step.
3) **The DRS probe should be static during measurements.** Rotation and translation of the DRS probe is not preferable since this is prone to inducing additional noise into the DRS signal.
4) **Maintain contact between the DRS probe and tissue during optical measurement.** Without direct contact between the DRS probe and the bone tissue, the DRS probe is prone to measure noise. For instance, an air gap between the tissue and probe could influence the DRS spectrum.
5) **The actuating mechanism must be able to actuate the probe tip to a minimum actuating depth of 100 mm, with respect to the entrance point of the vertebrae.** To test the sensor, the system should be able to drive the tip from the entrance point through the pedicle to the cortical bone of the anterior side of the vertebra. To determine the maximum distance along the line of actuation, Pythagoras combined with the values from Zhoul et al.[25] were used. The maximum upper vertebra depth (UVD) was 32.7 mm, the maximum lower vertebra depth (LVD) was 47.8 mm and the maximum width of the vertebra (VW) was 117.8 mm shown in figure 1. This results in a maximum distance of 99.8 mm, thus a minimum actuation depth of 99.8 mm.[25]

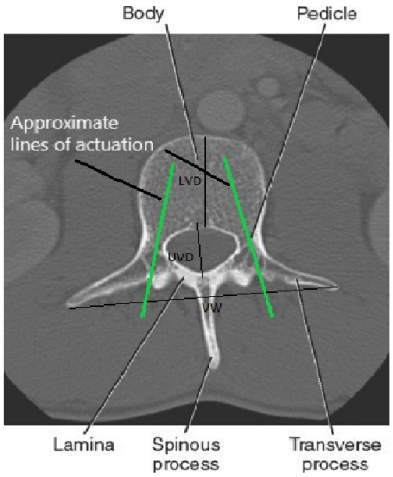

Fig. 1. Reference of a vertebra showing terminology, and lines of actuation used to determine maximum actuation dept. VW is width of the vertebra, LVD is the lower vertebra depth and the UVD is the upper vertebra depth. [26]

6) **The DRS probe should not break.** From hands on testing it was estimated that the DRS probe is prone to buckle because of its slender geometry. The optical fibers that run through the probe could also be pushed back into the metal rod encasing. The axial load that the probe can bear is unknown and cannot be tested or simulated because of uncertainties. Therefore the requirement is to optimally protect and encase the probe.

B. Fixation

1) **The relative displacement between the vertebra and the screw tip must not exceed 1.65 mm at point of**

initial insertion. The relative displacement between the vertebra and the screw is limited by the pedicle width and the probe tip diameter, because the probe tip is required to stay inside the pedicle to avoid inaccurate measurements. The pedicle width of the cervical vertebrae are the smallest ($\pm$ 5 mm)[3], so the maximum displacement should be half the pedicle width (2.5 mm) minus the radius of the sensor tip (.85 mm).

2) **A segment of five porcine vertebrae must be fixated.** The tests for validating the DRS probe will be performed on a porcine vertebra, which will be supplied in segments of five vertebrae.
3) **The rotating angle about spinous process/ longitudinal axis must be 90 degrees.** The actuating mechanism should be able to actuate the probe in line with any of the pedicles. Because a segment of five vertebrae will be used, the adjustable angle about the longitudinal axis is important for aiming the actuation. This longitudinal angle of the pedicles variate with the anatomy of vertebra and ranges between -5 degrees and 45 degrees [27] (see figure 2), so the total rotating angle should be 90 degrees.

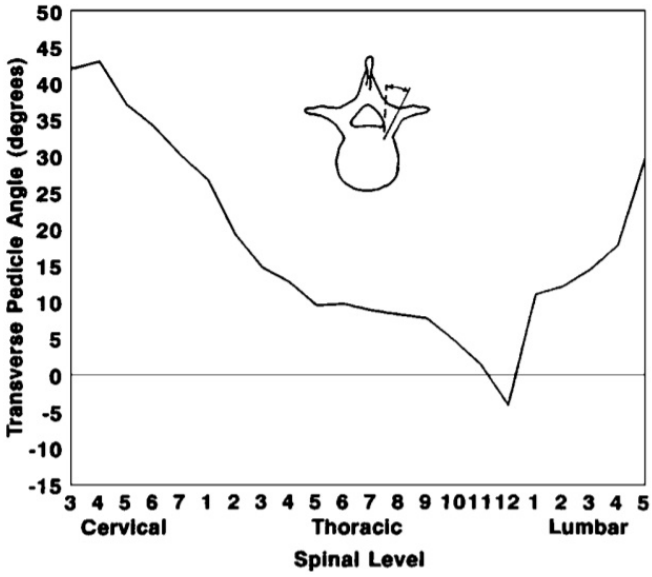

Fig. 2. The longitudinal angle of the pedicle plotted against the spinal level of the vertebra. [27]

C. Non-functional

1) **The actuating mechanism should be able to do 100 cycles according to specification.** The purpose of the actuation mechanism needs to be taken into account. The actuation mechanism will be used to perform validation experiments for the DRS sensor. For this validation, at least 100 operational cycles, which is a complete insertion of the screw, are required.
2) **The distance measurement should be recordable.** During the DRS probe validation, the insertion distance of the DRS probe in the vertebra is to be recorded.

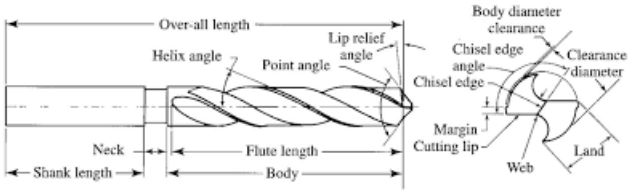

Fig. 3. Two-Flute twist drill geometry, showing the web and flutes.[29]

II. Design

In this chapter the design decisions are explained for different functions of the system.

A. Guidance mechanism

Two working principles were identified suitable for guiding the DRS probe into the vertebra. The first working principle removes bone material by drilling and the second working principle consists of screwing, thereby pressing the bone material aside. For both working principles the center of the drill or screw will be cannulated by a 1.7 mm diameter shaft, so the probe can be implemented. Figure 3 shows a normal drill bit that consists of a solid web which forms the center of the bit, adjoined by flutes (needed for material expulsion) that spiral around the web. To maintain central stability in the drill or screw, the hole in the center of the shaft should at least not be greater than the diameter of the solid center. For a normal drill bit, the solid center (web) is about 10% of the outer diameter [28] while for a normal wood screw, the solid center is about 70% of the thread diameter (by DIN571). Considering a maximum screw diameter of 7 mm used in a surgical work flow, a normal drill cannot be used for the probe implementation. Concluding, either a specifically fabricated drill with a larger web or a normal screw are to be used in the system. Because of time limitations, manufacturing limitations, and to reduce overall system complexity the screwing concept was chosen as a guidance mechanism.

For screwing, the vertical translation is coupled to, and induced by, the screw pitch. However, an axial force is required to let the tip of the screw gain traction in the material during initial insertion and to prevent slippage that is most likely to occur during first part of the insertion, because the contact area of the screw with the material is still relatively small. From previous research, taking a one sided 95% confidence interval, it is known that a maximum torque of 2.2 Nm[30] is needed and the rotation speed is usually relative low, around 15 RPM.[31] No existing study was found on the correlation between screw dimensions, torque and axial force. A study conducted by Hausmann et al. [32] measured the axial force needed to drive four different screws into two stacked sawbones while measuring the compressive force in between the two bones. The properties of sawbone are similar to those of real bone.[33] The results of the test with the cannulated AO screw will be used to estimate the axial force needed to drive a range of pedicle screws into bone. Using scaling, the range of maximum force required to

drive a screw into sawbone for screws of 4.5-7 mm diameter was estimated to be 43-104 N, at respectively 31-20 RPM.

The axial force could be induced by a pneumatic actuator or an electronic motor with a spindle. Since 200 N is the axial force used for drilling[34] and the maximum axial force for screwing was estimated at around 100 N for a 7 mm diameter screw, the maximum required axial force was chosen at 200 N. Furthermore, the force also needs to be applied in static position during DRS measurement, otherwise an air gab could develop between the tip of the probe and the tissue. These specifications taken into account, it can be concluded that the pneumatic actuator is best suited because the pneumatic actuator generates a constant force over the complete stroke and the force is independent of the translation speed. Also, an electronic motor could potentially overheat while no translation is induced but an axial force is still being generated.

Finally, a guided drive (linear guidance and pneumatic actuator combined) was chosen with a stroke of 100 mm and maximum force of 200 N, namely the FESTO DFM-16-100-P-A-KF shown in figure 5 at number 2. The main reason for choosing a combined guidance and actuation system is to reduce the amount of backlash. The total tolerable amount of displacement defined in requirement B1 is 1.65 mm, this includes backlash. The deflection of the guided drive at the full stroke of 100 mm is 0.01 mm due to bearing clearance. Furthermore the maximum allowable torque on the guided drive in line with the screwing direction is 19 Nm. This offers an estimated safety factor of 10.

B. Screw

To meet the requirements, there should be no relative translation between screw and probe and for optional continuous measurement there should be no relative rotation between the probe and vertebra during actuation. To circumvent rotation of the probe it has to be implemented in the centre of the screw, which implicates using a cannulated screw that has also been mentioned before. Regarding future application and the material reaction on the properties of bone, using pedicle screws would be preferable. However the inner diameter of the available cannulated screws were too small for the probe to fit, so they needed to be drilled to a larger diameter. Unfortunately, the titanium pedicle screws could not be machined with the tools in the available machine shop.

Since the material of the pedicle screw is not specified a pedicle screw with a fixed head would be favourable, it was chosen to machine a screw based on a wood thread bolt. Wood thread bolts have a thread pitch (2.8 mm) that is similar to the pitch of pedicle screws (2.6 mm).

Normal drill bits can drill ten times their diameter, a special drill bit was found which could drill 60 mm at a diameter of 2.5 mm (largest probe diameter: 2.3 mm). To achieve a higher overall screw length, the screw is drilled into from two sides. Because a drill is always slightly acentric, it was expected that drilling a 60 mm, 2.5 mm hole from both sides would result in offset holes at the connecting point. Instead a combination of a 60 mm, 2.5 mm hole from one side and a shallower hole from the other side was chosen. For the diameter of the shallower hole, a diameter close to that of the tip of the probe (1.68 mm) was preferred to block material from entering into the space between the probe and the screw, therefore a 1.7 mm diameter was chosen. Following the nominal drill rule[35], a 17 mm deep hole could be drilled. Adding up both hole depths, the achievable overall screw length would be 77 mm. To be able to attach the screw to the system, the end of the screw has a straight 15 mm shaft. For determining the thickness of the wood thread bolt, a static study of a 5 mm wood thread bolt, showed that a torque of 2.2 Nm would induce screw failure. A study of a 6 mm wood thread bolt with the same torque applied, showed a maximum induced stress of 490 MPa, which is less than the yield stress of normal steel. A 6 mm wood-screw was therefore chosen, displayed in figure 5 at number 4.

C. Rotation and transmission

For screw rotation, a DC motor and a stepper motor were considered. The requirement for rotation is to rotate highly controlled, because translation is determined by the rotation. It is also important to stop after every step, to fulfill requirement A3.

With these specifications taken into account, the stepper motor is more suited compared to the DC motor. The stepper motor can be easily controlled, for small and precise rotations. The stepper motor is shown in figure 5 at number 3.

Ideally the stepper motor and the screw are directly linked, so no transmission is needed. Because the DRS probe is positioned in the centre of the screw, a hollow stepper motor would be necessary to avoid a mechanical transmission. Slippage is also minimal without using mechanical transmission. However, the height of the hollow stepper motor is the limiting factor because the DRS probe, with its fixed usable length of 178 mm, should then go through the the hollow stepper motor and the screw. The screw will be 77 mm long and therefore the maximum length of the stepper motor calculates to 100 mm, with the probe extending 1mm from the screw. A torque of 2.2 Nm of the stepper motor is at least required, as explained before. Hollow stepper motors that would suffice, start at a height of 114 mm. [36] Consequently it is not possible to use a hollow stepper motor in our design, so a transmission will be used.

For the transmission a belt-drive was chosen, because belt-drives have no backlash when tension is applied correctly. Furthermore, it is easier to align them compared to gears. Two pulleys were selected with a ratio close to 1:2, therefore the stepper motor needs to deliver 1 Nm torque. The holding torque of stepper motors is higher than the running torque, so the the holding torque needs to be more than 1.1 Nm. A stepper motor was selected with 1.5 Nm holding torque and a running torque of 1.2 Nm at 100 steps/second.

Because a mechanical transmission is used, a screw bit was designed to transmit torque from the pulley to the screw. The screw bit is made from a steel rod with a slide fit hole at the lower end to clasp the upper shaft of the screw and has two bearings at the upper and lower part of the bit to minimize play. Slide bearings were used because of the relatively low rotation speed. An aluminum plate with a thickness of 10 mm is used to attach all other parts. On this plate the pneumatic actuator, stepper motor, mechanical transmission and DRS probe fixation system are attached.

D. Distance sensor

The distance needs to be measured with an accuracy that is greater than the stepsize of the actuator. This way it can be a controlled actuation. There were multiple options as distance measurement. A laser sensor was chosen, since it was available and accurate enough.

The laser sensor will measure distance to the aluminum plate and therefore represents the actuation depth of the DRS probe. The deflection of the plate could introduce a measurement error, but with an approximately constant axial force produced by the pneumatic cylinder during screwing, the deflection is constant over the full insertion, making the DRS probe actuation depth equal to the distance measured by the laser sensor.

The laser sensor, an optoNCDT 1420 ILD1420-100, has a measuring range of 50 - 150 mm, which is more than the actuation depth available by the amount of thread on the screw. The laser sensor has a resolution of 4 μm. The location of the sensor should be 50 mm above the ultimate point of retraction of the cylinder, because the measuring range starts from 50 mm.

E. Control

The mechatronic part of the actuating system consists of the following parts: an Arduino uno, a National Instruments data acquisition system (DAQ), a laser sensor, a stepper motor controlled with a leadshine m542 stepper motor driver. Furthermore the laser sensor generates an output current which is linearly dependent to the distance measurement, 4 mA relates to 50 mm and 20 mA relates to 150 mm. To convert this output current into a voltage a resistor (540Ω) was used to create a voltage range between 2 V and 10 V.

The used DAQ from National Instruments measures this voltage with an analog 16 bit input ports with a voltage range of -10 to 10 volt. Before passing it on to the Arduino, via two analog 16 bit output ports with a voltage range of -10 to 10 volt, the 100 mm range of the sensor is divided into two intervals by the DAQ and consequently, the Arduino uses two analogically reading pins of to achieve a higher resolution. The first pin represents the first 50 mm (50 - 100 mm) of the measuring range. The second pin represents the second 50 mm of the measuring range (100 - 150 mm).

The Arduino measures the value from the DAQ and converts it into a 10 bit digital signal. This value is used to implement control through the Arduino. The final precision will be dominated by the resolution of the Arduino's ADC, because the precision of the laser sensor is approximately 10 times higher than the resolution of the Arduino's ADC. The analog pins of the Arduino has a voltage range from 0 - 5 V and the Arduino has a 10 bit ADC, consequently the resolution of the Arduinos ADC is 100 mm / 2048 = 0.049 mm interval (two pins are used).

F. Vertebra fixation

The vertebra fixation for this system will be designed for a segment of five interconnected vertebrae. The segment needs to be fixated to drive the DRS probe in with as little relative motion to the system as possible. Since it is unknown what the segment will look like exactly, a reference frame was formed from literature, for which the fixation should be designed for (see figure 4). The vertebrae could originate from different parts of the spine, thus the shapes and sizes of vertebrae will differ. Also, it is likely that the vertebrae are covered in soft tissue, which could vary in thickness and condition. The slipperiness of the tissue around the vertebrae will make a friction locked fixation more difficult.

Fig. 4. Spine used to form a reference frame for the fixation design. [37]

Two fundamental different working principles where explored, namely fixating the segment by clamping the vertebrae with tension or by applying compression on the surface of the vertebrae. The tension working mechanism was focused on attaching hooks or sutures to the soft tissue and herewith pulling it down onto a bottom structure. However this working principle is dependent on the quality and availability of the soft tissue, which could vary due to the condition of the specimen and is preferably cut away. Using compression, the segment is fixated by putting pressure on concentrated spots of the segment, consequently the quality and the amount of soft tissue are less important. Compressing the segment is therefore more adjustable to different specimens. Therefore a compression based fixation was used in the final design. The final design contains a vice, attached to a clamp base on which 3D printed clamps are mounted (see figure 5 number 1). These clamps contain pins that can fixate the system from different angles and positions, which makes it a form locked fixation. However the pins also exert compressive force on the vertebra, because the pins can be wind up by their screwing thread and the nuts inside the clamp. The ends of the pins are made to enter through the tissue around the vertebra or even through the cortical bone.

G. Frame

The finally described part of the actuating system is the frame, which connects the vertebra fixation to the actuating part of the design. The frame needs to resist the previously discussed reaction forces, generated by the screw insertion, causing minimal deflection. Furthermore, the frame must allow the vertebra fixation to be flexible in positioning. The insertion point of the screw must be adaptable over at least the maximum human spinal width (117.8 mm) and the maximum human pedicle height (20 mm).[3] Also the height of the actuation part must be adjustable to the different vertebra heights. In the final design a bridge shaped frame is chosen, because this is in favor of minimizing deflection. With an axial force of 200 N a maximum deflection (<0.01 mm) of the bridge was calculated. The frame was assembled by aluminum extrusion profiles that are; stiff, light weighted, quickly assembled, and easily adaptable to the various insertion points. The frame has a width of 330 mm, length of 340 mm, and a height of 540 mm, reaching all possible insertion points. The final design is displayed in figure 5, the frame is labelled with number 5.

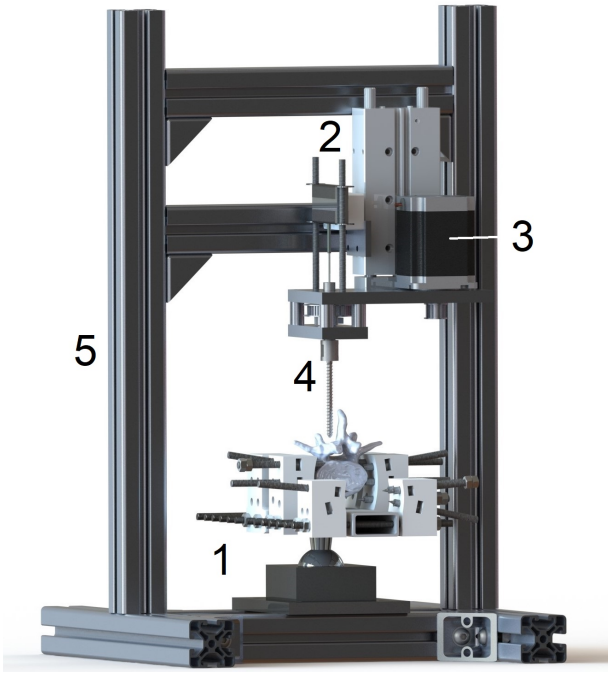

Fig. 5. A complete overview of the final actuation system design

III. Validation

To test if the actuation mechanism satisfies the requirements, a validation procedure was created. The validation is performed through a set of seven tests, each test will be described and the corresponding requirements will be linked.

A. Test 1; Relative motion

The first test was executed to validate requirement B1, which describes the potential displacement of the screw, perpendicular to the screwing direction. This relative displacement between the vertebra and the screw consists of a combined displacement of both the vertebra itself and that of the screw. Since maximum displacement will occur at the tip of the screw and the vertebra is assumed to be fixed rigidly to the clamp, this test can be divided into the following sub tests:

- What is the amount of displacement, perpendicular to the screwing direction, of the vertebra clamp?
- What is the amount of displacement, perpendicular to the screwing direction, of the tip of the screw?

For both tests, a spring balance was used to apply load perpendicular to the screwing direction in discrete steps of 2.5 N to a maximum of 10 N. For the first test, load was applied on the clamp. For the second test, load was applied on the screw tip. For both scenarios, displacement was measured five times with a dial gauge (resolution of 0.01 mm).

B. Test 2; Rotating angle

The following test was performed to validate requirement B3:

- What is the maximum insertion angle about the longitudinal axis/ spinous process?

A protractor (resolution of 0.5 degrees) was used to measure the deviating angles (tilted to both sides) of the vertebra from the upright position about the longitudinal axis. Both angles were measured five times and added up.

C. Test 3; Actuation dept

This test was performed to validate requirement A5, which covers the insertion depth of the screw tip:

- What is the maximum actuation dept of the screw?

Several 3D printed human vertebrae from different levels of the spine ($T4$, $C4$, $L1$, $L5$) were used as a reference. The screw tip was positioned at the point of insertion whilst fully retracted, and actuated until further actuation was obstructed. For each of those vertebrae, the final actuation dept was measured. This measurement was repeated three times per vertebra.

D. Test 4; minimum pressure

The next test was conducted to validate requirement A6, which is dedicated to not breaking the probe. Although this is a qualitative requirement, an initial load on the DRS probe can be estimated. Since the pressure can be adapted to adjust the axial load, the amount of axial force required to drive the screw without the probe can be measured. During initial insertion, the load encountered by probe can be fully accounted to this pressure, since the thread of the screw has not gained traction.

- What is the minimal axial force required to gain screwing traction in the testing material?

The minimally required axial pressure was determined over a full screw insertion. The screw was rotated at a constant speed and the pressure was increased until the screw visually

translated. The screw was inserted in a cancellous bone like tissue (PU foam, ρ = 259 kg/m^3), with a similar compressive strength property compared to real bone.[38] This test was executed for three different rotational speeds of the screw (25.5, 51, 75 RPM), both with and without pilot holes and repeated three times.

E. Test 5; Static probe

This test was performed to validate requirement A3, which claims that the probe should be static during measurement to avoid measurement noise. Uncontrolled and/or unwanted translation while the stepper motor is static but the cylinder is actuated should be avoided. Therefore, the pressure at which translation occurs was determined.

- At what pressure does translation occur without rotation of the stepper motor?

The pressure was increased in discrete steps of 0.5 bar until translation in the cancellous bone like tissue (PU foam, ρ = 259 kg/m^3) was measured by the laser distance sensor, repeated three times.

F. Test 6; Step size

The following test was performed to validate requirement A2:

- What is the smallest controllable step size in the testing material?

While actuating ten steps in the cancellous bone like material (PU foam, ρ = 259 kg/m^3) with intended step sizes of 1, 0.8, 0.5, 0.3, 0.2, and 0.1 mm, the achieved step size was measured each step.

G. Test 7; Maintaining contact

This test was executed to validate requirement A4. This requirement states that there should be contact between the tissue and the DRS probe during measurement, which could be determined by DRS measurements. The amount of DRS measurement noise was studied by comparing a static reference to a step wise, and a continuous probe insertion.

- Is the reference probe spectrum (containing fat) similar to the actuated probe spectrum?
- Does a continuous actuation generate a comparable static measurement?

A static reference DRS measurement was compared to a measurement recorded during ten discrete steps of actuation, both inserted in butter.
Secondly, continuous insertions in butter were compared to a static reference. Ten static and 22 continuous measurements were done using the DRS probe.

IV. Data analysis

In this section the methodology in answering the validation questions by processing measurement results will be elaborated.
For test 1, a plot is given depicting each amount of applied force connected to the amount of displacement with a 95% confidence interval (the clamp displacement summed with the screw tip displacement). A data fit was made, which was used to distinguish deflection and backlash. Finally, a t-test was performed on the maximum displacement. to validate the requirement coupled to this test.
For test 2, the mean and standard deviation (sd) of the maximum rotation angle are calculated. To validate the associated requirement, a t-test was performed.
For test 3, the mean and sd were calculated for each vertebra from which the validation question could be answered. A t-test to prove that the coupled requirement is met was unnecessary, because there was a significant difference between the required value and the measured values. For test 4, the forces are given for a screw insertion with and without a pilot hole and for the given rotational speeds.
For test 5, the pressure on the pneumatic cylinder could not be determined, due to insufficient maximum pressured air availability.
For test 6, each step size is depicted in a plot with a 95% confidence interval. The minimum controllable step size is determined via a fit in the box plot. Two other lines are plotted, which represent acceptable error margins($-$ 10 an $+$ 5 percent of the step size). The step size that reaches between these limits is the smallest usable step size.
In test 7 the validation question is answered via a t-test, comparing the reference to the measured values.
For all the t-tests a hypothesis was set, a p-value was computed (p) , and a significance level of 0.05 was used. If p was below this significance level, the hypothesis was rejected.

V. Results

A. Test 1; Relative motion

Figure 6 describes the total displacement of the actuation system and the clamp at the corresponding load. For the highest applied force of 10 N, the average displacement is 0.78 mm, which is significantly lower compared to the 1.65 mm displacement($p < 0.001$) set in the requirements.

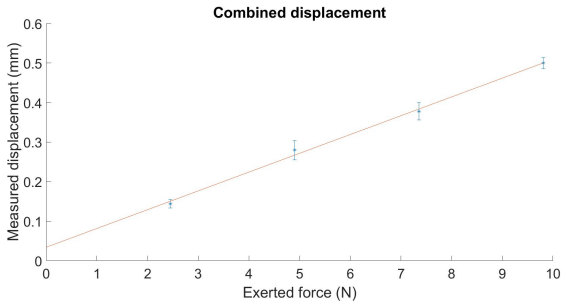

Fig. 6. A graph showing the combined displacement plotted against the applied force at the DRS sensor tip.

B. Test 2; Rotating angle

The mean maximum rotation angle and the sd were 98.5, and 1.5 degrees respectively. This is significantly higher ($p < 0.001$) compared to the 90 degrees mentioned in the requirements.

C. Test 3; Actuation depth

The maximum actuation depth of the screw in the vertebra was in the L5 vertebra [mean = 54.33 mm, sd = 3.00 mm], followed by the L1 [mean = 53.00 mm, sd = 0.48 mm], next the T4 [mean = 46.82 mm, sd = 2.00 mm] and minimum depth was achieved in the C4 [mean = 45.55 mm, sd = 0.22 mm].

D. Test 4; Minimum pressure

While using a pilot hole for insertion at a speed of 51 and 75 RPM, no axial force generated by the cylinder additional to the weight of the aluminum plate was needed to insert the screw into the material. At 25.5 RPM the pneumatic cylinder needed to deliver 10 N. Without a pilot hole a force of 141 N was required at 25.5 and 75 RPM, and a force of 131 N at 51 RPM. The forces were computed from the cylinder pressure and diameter (16 mm). For all insertions the weight of the stepper motor combined with the plate was 29 N.

E. Test 5; Static probe

No translation occurred into bone like material when the maximum pressure [7 bar] was applied.

F. Test 6; Step size

Figure 7 depicts an increasing absolute (and relative) error with a decreasing step size. The set step sizes were 0.05 mm [mean = 0.056 mm, sd = 0.032 mm], 0.1 mm [mean = 0.104 mm, sd = 0.021 mm], 0.2 mm [mean = 0.199 mm, sd = 0.016 mm], 0.3 mm [mean =.288 mm, sd = 0.018 mm], 0.5 mm [mean = 0.491 mm, sd = 0.019 mm], 0.8 mm [mean = 0.799 mm, sd = 0.009 mm], and 0.975 mm [mean = 0.984 mm, sd = 0.005 mm]. The green lines indicate the predetermined error margins, if the 95% confidence interval of the measurements falls within the green lines the set step size meets the set maximum error criteria. All the measured set step sizes higher than 0.5 mm meet the maximum error criteria.

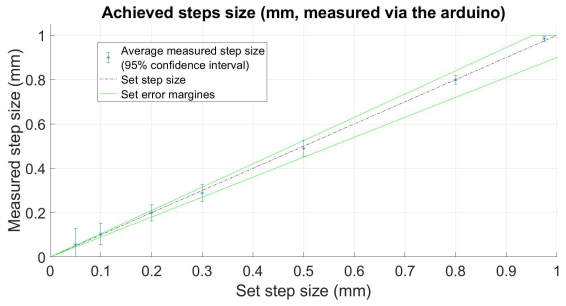

Fig. 7. A graph showing the average achieved step with a 95% confidence interval and and accepted error margins plotted against the set step size

G. Test 7; Maintaining contact

The amount of fat [mean = 84.8%, sd = 0.9%] measured with a static DRS probe is the same as ($p = 0.154$) the amount of fat [mean = 85.4%, sd = 1.2%] measured with the step wise inserted DRS probe positioned in the actuation mechanism. The measured amount of fat during conctinous actuation [mean = 83.8%, sd = 0.8%] is significantly smaller ($p = 0.0076$) than the amount of fat in the static reference.

Requirements A1, C1, and C2 are not validated because they describe trivial aspects of the design. B2 was not yet validated due to no availability of a porcine spine.

VI. Discussion

In this design study we explored options for inserting a DRS probe into a segment of vertebrae. The system facilitates validation of the DRS probe, and ultimately could prevent screw misplacement during spinal surgery. A final design was fabricated and validated on the set requirements.

Results

From test 1 can be concluded that requirement B1 is met up to a maximum lateral force of 10 N. This maximum was set because simulations showed a high probability of screw deformation and only one screw was available for testing. Moreover, the behavior of the screw can only be estimated. For example, changing the insertion angle during insertion will cause high lateral forces, especially if insertion is continued.

To accurately determine the displacement during insertion, an insertion in bone should be recorded using X-ray. Subsequently, the maximum displacement could be determined through increasing the insertion angle up to screw failure.
From figure 6 an expected linear correlation between deflection and load can be assumed. If the displacement merely consists of deflection, the linear data fit would be expected to show no displacement when no load is applied. However, the fit in figure 6 shows a displacement when no load is applied. This offset in the figure could be interpreted as the backlash of the clamp combined with the backlash of the screw. Presumably the backlash of the system is mainly caused by the sliding bearings. Ball bearings could be used to lower the backlash, because they have a tighter fit. Presumably, no backlash exists between the the vertebra and the clamp, because the clamp can be adjusted to the shape of the vertebra. However, deformation of the vertebra could induce deflection of the screw which was not measured and would have to be measured on real vertebrae.
From test 2 can be concluded that requirement B3 was met. However, it is relatively challenging to position the vertebra in the desired actuation direction, because the angle of the ball joint cannot be monitored. This could be improved to facilitate more precise aiming for insertion. Furthermore, the system is not suitable for tests on living organisms because the aiming and fixating would have to be redesigned.
The actuation depths resulting from test 3, do not meet requirement A5. However, the screw was inserted all the way through any of the 3D printed vertebrae, as well through the biggest vertebra ($L5$) that was used. Moreover, the test used a vertically positioned spine, whereas the requirement was based on a tilted screw insertion. Furthermore, requirement

A5 combined maximum dimensions(UV,UVD,LVD) of different vertebrae. Therefore, the required insertion dept might be set to high.

The exerted axial force found in test 4 combined with the weight of the stepper motor and moving plate, gives a range of 160 N to 170 N to insert the screw into PU foam. This is more than the force estimated in II-A. Test 4 also showed that using a pilot hole lowers the total axial force to 30 - 40 N. Presumably, a pilot hole enables the thread of the screw to gain traction in the material, this implicates that the axial force exerted through the thread of the screw is about 130 N. No clear correlation between the rotational speed of the screw and the required pressure was found. Although the requirement of not breaking the probe can not be answered, this test gives some important insights. The measured range of axial force is likely to exist during the full length of insertion, because the material has to be compressed in a similar manner be it now largely accounted to the torque of the stepper motor. Therefore the combined axial load on the probe and screw estimates to 160 N to 170 N. The probe was not tested in PU foam, because the material might be tougher than bone tissue which would unnecessarily deform the probe.

From test 5 we can conclude that translation without rotation occurs above 7 bar in the PU foam. Due to insufficient pressured air availability, the exact pressure could not be determined. So can be concluded that translation in the PU foam only occurs aided by rotation of the screw, because the required externally applied pressure to insert a screw is 7 bar. Therefore, requirement A3 is met for the PU foam.
From figure 7 can be concluded that a step size larger than 0.5 mm satisfies the predetermined error criteria of $+5$ and -10%. Hereby requirement A2 is met, because the minimum step size is less than 1 mm. Depending on acceptable error margins, the minimum accepted step size could be adapted. At error margins of at least $+$ 0 and $-$ 3%, the requirement of a 1 mm step size is met using a 95% confidence interval of the measured step size.
The results of test 7 show no significant difference between the mean fat percentages of the reference and the step wise insertion, thus can be assumed that the actuation mechanism does not influence the DRS signal.

The continuous DRS measurement, shows a significantly smaller mean fat percentage compared to the reference. However, the measured difference in fat percentage is mostly constant: the standard deviation varies 0.124 % fat between the two data sets, while the average of the two data sets differs by 1.1 % fat. Considering the relatively constant deviation, DRS measurement during actuation is assumed plausible if this deviation is taken into account. Requirement A4 was assumed to be validated by these results, however the behaviour of butter presumably differs from bone and should therefore be revalidated on bone tissue.

Design iteration

Drilling could be a good alternative for guiding the DRS probe during insertion. The principle of screwing was chosen for reasons explained before. Although cannulated medical bone drill bits[39] exist, the DRS probe did not fit in these drills. Also, these bone drills have relatively shallow flutes to extrude excess material and is the force and torque involved therefore expected to be higher with a higher risk of failure. [40] For medical application, drilling probably gives a better possibility for a directional correction, due to the smaller diameter of the drill bit compared to the screw. Also do repositioned pedicle screws have less original grip.[41] Therefore, drilling could be argued better suited for medical application. On a general note, for surgical implementation the system should provide feedback to the surgeon and have certain emergency stops. Furthermore the work-flow for the surgeon should be made intuitive.

The mechatronics system was build upon mostly available components, which leaves some room for improvement for a design iteration of this part of the system. It is recommended to eliminate the arduino from the mechatronic system and implement direct control of the stepper motor through a data acquisition system (with a resolution of more than 11 bit in a 2 to 10 volt range). This will improve the resolution of the measurement allowing for more precise control. Secondly, a driver allowing for full stepping is recommended, increasing available motor torque by approximately 29%. Thirdly, an electronically controlled pressure valve could be used to implemented the exerted pressure in the control loop resulting in fully automated insertion.

VII. Conclusion

The system will be used for validating the DRS probe on segments of a couple of vertebrae. In conclusion the system has achieved the following most important specifications:

- At error margins of at least $+$ 0 and $-$ 3%, the requirement of a 1 mm step size is met.
- There was no significant difference noted between the mean fat percentages a reference fat measurement compared to a step wise insertion through the actuation system.
- For the applied lateral force of 10 N, the average deflection of actuation is measured 0.78 mm, compared to the 1.65 mm displacement set in the requirements ($p < 0.001$).
- The estimated maximum load on the probe and screw is 170 N, it was not tested if the probe would fail under this load.

Therefore can be concluded that we achieved the design goal and the actuation system can be used for validation of the DRS probe, so the next step should be to test the actuation system on real bone.

REFERENCES

[1] S. Rajaee, H. Bae, L. Kanim, and R. Delamarter, "Spinal fusion in the united states: analysis of trends from 1998 to 2008." *The Spine Journal*, vol. 37, no. 1, pp. 67–76, 2012.

[2] R. W. Gaines Jr, "The use of pedicle-screw internal fixation for the operative treatment of spinal disorders," *JBJS*, vol. 82, no. 10, pp. 1458–1476, 2000.

[3] I. Busscher, J. J. Ploegmakers, G. J. Verkerke, and A. G. Veldhuizen, "Comparative anatomical dimensions of the complete human and porcine spine," *European Spine Journal*, vol. 19, no. 7, pp. 1104–1114, 2010.

[4] J. N. Weinstein, B. L. Rydevik, and W. Rauschning, "Anatomic and technical considerations of pedicle screw fixation," *Clinical Orthopaedics and Related Research®*, vol. 284, pp. 34–46, 1992.

[5] J. M. Hicks, A. Singla, F. H. Shen, and V. Arlet, "Complications of pedicle screw fixation in scoliosis surgery: a systematic review," *Spine*, vol. 35, no. 11, pp. E465–E470, 2010.

[6] C. J. Schulze, E. Munzinger, and U. Weber, "Clinical relevance of accuracy of pedicle screw placement: a computed tomographic-supported analysis," *Spine*, vol. 23, no. 20, pp. 2215–2220, 1998.

[7] W. H. M. Castro, H. Halm, J. Jerosch, J. Malms, J. Steinbeck, and S. Blasius, "Accuracy of pedicle screw placement in lumbar vertebrae," *Spine*, vol. 21, no. 11, pp. 1320–1324, 1996.

[8] Y. J. Kim, L. G. Lenke, K. H. Bridwell, Y. S. Cho, and K. D. Riew, "Free hand pedicle screw placement in the thoracic spine: is it safe?" *Spine*, vol. 29, no. 3, pp. 333–342, 2004.

[9] R. Verma, S. Krishan, K. Haendlmayer, and A. Mohsen, "Functional outcome of computer-assisted spinal pedicle screw placement: a systematic review and meta-analysis of 23 studies including 5,992 pedicle screws," *European Spine Journal*, vol. 19, no. 3, pp. 370–375, 2010.

[10] H. C. Sagi, R. Manos, R. Benz, N. R. Ordway, and P. J. Connolly, "Electromagnetic field-based image-guided spine surgery part one: results of a cadaveric study evaluating lumbar pedicle screw placement," *Spine*, vol. 28, no. 17, pp. 2013–2018, 2003.

[11] P. Merloz, J. Troccaz, H. Vouaillat, C. Vasile, J. Tonetti, A. Eid, and S. Plaweski, "Fluoroscopy-based navigation system in spine surgery," *Proceedings of the Institution of Mechanical Engineers, Part H: Journal of Engineering in Medicine*, vol. 221, no. 7, pp. 813–820, 2007.

[12] A. Manbachi, R. S. C. Cobbold, and H. J. Ginsberg, "Guided pedicle screw insertion: techniques and training," *The spine journal*, vol. 14, no. 1, pp. 165–179, 2014.

[13] E. Ron, "Cancer risks from medical radiation," *Health physics*, vol. 85, no. 1, pp. 47–59, 2003.

[14] R. Härtl, K. S. Lam, J. Wang, A. Korge, F. Kandziora, and L. Audigé, "Worldwide survey on the use of navigation in spine surgery," *World neurosurgery*, vol. 79, no. 1, pp. 162–172, 2013.

[15] A. Swamy, G. Burström, J. W. Spliethoff, D. Babic, C. Reich, J. Groen, E. Edström, A. E. Terander, J. M. Racadio, J. Dankelman *et al.*, "Diffuse reflectance spectroscopy, a potential optical sensing technology for the detection of cortical breaches during spinal screw placement," *Journal of biomedical optics*, vol. 24, no. 1, p. 017002, 2019.

[16] K. Kim, J. Lee, W. K. Chung, S. Choi, Y. S. Kim, and I. H. Suh, "A noble bilateral teleoperation system for human guided spinal fusion," in *Proceedings 2007 IEEE International Conference on Robotics and Automation*. IEEE, 2007, pp. 940–946.

[17] J. Lee, K. Kim, W. K. Chung, S. Choi, and Y. S. Kim, "Human-guided surgical robot system for spinal fusion surgery: Corass," in *2008 IEEE International Conference on Robotics and Automation*. IEEE, 2008, pp. 3881–3887.

[18] J. J. Santos-Munné, M. A. Peshkin, S. Mirkovic, S. D. Stulberg, and T. Kienzle, "A stereotactic/robotic system for pedicle screw placement," *Proceedings of the Medicine Meets Virtual Reality III*, pp. 326–33, 1995.

[19] G. B. Chung, S. G. Lee, S. Kim, B.-J. Yi, W.-K. Kim, S. M. Oh, Y. S. Kim, J. I. Park, and S. H. Oh, "A robot-assisted surgery system for spinal fusion," in *2005 IEEE/RSJ International Conference on Intelligent Robots and Systems*. IEEE, 2005, pp. 3015–3021.

[20] H. Jin, P. Zhang, Y. Hu, J. Zhang, and Z. Zheng, "Design and kinematic analysis of a pedicle screws surgical robot," in *2010 IEEE International Conference on Robotics and Biomimetics*. IEEE, 2010, pp. 1364–1369.

[21] T. Ortmaier, H. Weiß, U. Hagn, M. Grebenstein, M. Nickl, A. Albu-Schaffer, C. Ott, S. Jorg, R. Konietschke, L. Le-Tien *et al.*, "A hands-on-robot for accurate placement of pedicle screws," in *Proceedings 2006 IEEE International Conference on Robotics and Automation, 2006. ICRA 2006.* IEEE, 2006, pp. 4179–4186.

[22] R. Oftadeh, M. Perez-Viloria, J. C. Villa-Camacho, A. Vaziri, and A. Nazarian, "Biomechanics and mechanobiology of trabecular bone: a review," *Journal of biomechanical engineering*, vol. 137, no. 1, p. 010802, 2015.

[23] A. M. Richards, N. W. Coleman, T. A. Knight, S. M. Belkoff, and S. C. Mears, "Bone density and cortical thickness in normal, osteopenic, and osteoporotic sacra," *Journal of Osteoporosis*, vol. 2010, p. 5, 03 2010.

[24] K. Z. . K. S. S. Chahoud, J., "Surgical site infections following spine surgery: eliminating the controversies in the diagnosis," *Frontiers in medicine*, vol. 1, p. 7, 03 2014.

[25] S. H Zhou, I. D McCarthy, A. Mcgregor, R. R. H. Coombs, and S. Hughes, "Geometrical dimensions ,of the lumbar vertebrae - analysis of data from digitised ct images," *European spine journal : official publication of the European Spine Society, the European Spinal Deformity Society, and the European Section of the Cervical Spine Research Society*, vol. 9, pp. 242–8, 07 2000.

[26] L. Kelley and C. Petersen, "Sectional anatomy for imaging professionals," St Louis, 2007.

[27] R. J. Kowalski, L. A. Ferrara, and E. C. Benzel, "Biomechanics of the spine," *Neurosurgery Quarterly*, vol. 15, no. 1, p. 4259, 2005.

[28] D. Yu, "Main technical conditions of twist drill." [Online]. Available: http://www.tongyutools.com/title1/technology.htm

[29] A. Vijayaraghavan, "Automated drill design software," *Lab Manuf Sustain*, vol. 1, pp. 01–10, 2006.

[30] K. Matsukawa, Y. Yato, T. Kato, H. Imabayashi, T. Asazuma, and K. Nemoto, "In vivo analysis of insertional torque during pedicle screwing using cortical bone trajectory technique," *Spine*, vol. 39, no. 4, pp. E240–E245, 2014.

[31] J. S. Kim, S. H. Choi, S. K. Cha, J. H. Kim, H. J. Lee, S. S. Yeom, and C. J. Hwang, "Comparison of success rates of orthodontic miniscrews by the insertion method," *The Korean Journal of Orthodontics*, vol. 42, no. 5, pp. 242–248, 2012.

[32] J. Hausmann, W. Mayr, E. Unger, T. Benesch, V. Vcsei, and C. Gbler, "Interfragmentary compression forces of scaphoid screws in a sawbone cylinder model," *Elsevier*, vol. 2007, no. 38, p. 763768, 2008. [Online]. Available: http://doi.org/10.1016/j.injury.2006.11.002

[33] E. A. Melamed, L. C. Schon, M. S. Myerson, and B. G. Parks, "Two modifications of the weil osteotomy: analysis on sawbone models," *Foot & ankle international*, vol. 23, no. 5, pp. 400–405, 2002.

[34] T. MacAvelia, M. Salahi, M. Olsen, M. Crookshank, E. H. Schemitsch, A. Ghasempoor, F. Janabi-Sharifi, and R. Zdero, "Biomechanical measurements of surgical drilling force and torque in human versus artificial femurs," *Journal of Biomechanical Engineering*, vol. 134, no. 12, p. 124503, 2012.

[35] F. D. Jones, E. Oberg, and H. L. Horton, "Machinery's handbook," Industrial Press, Incorporated, Tech. Rep., 2004.

[36] "Nema 23 bipolar 3nm (425oz.in) 4.2a 57x57x114mm 4 wires stepper motor cnc." [Online]. Available: https://www.omc-stepperonline.com/nema-23-bipolar-3nm-425ozin-42a-57x57x114mm-4-wires-cnc-step\per-motor-23hs45-4204s.html

[37] "Making back surgery safer," 2018. [Online]. Available: https://www.eurekalert.org/multimedia/pub/168914.php

[38] V. Shim, J. Boheme, C. Josten, and I. Anderson, "Use of polyurethane foam in orthopaedic biomechanical experimentation and simulation, polyurethane, fahmina zafar and eram sharmin," *IntechOpen*, august 2012. [Online]. Available: https://www.intechopen.com/books/polyurethane/use-of-polyurethane-foam-in-orthopaedic-biomechanical-experiment\ation-and-simulation

[39] N. Bertollo and W. R. Walsh, "Drilling of bone: practicality, limitations and complications associated with surgical drill-bits," in *Biomechanics in applications*. IntechOpen, 2011.

[40] F. R. Ong, "Analysis of bone drilling characteristics for the enhancement of safety and the evaluation of bone strength," Ph.D. dissertation, © Fook Rhu Ong, 1998.

[41] D. W. Polly Jr, J. R. Orchowski, and R. G. Ellenbogen, "Revision pedicle screws: bigger, longer shims-what is best?" *Spine*, vol. 23, no. 12, pp. 1374–1379, 1998.